

1 **An effective and efficient method for identification of contamination sources**
2 **in water distribution systems based on manual grab-sampling**

3
4 **Yiran Ji¹, Feifei Zheng², Jiawen Du³, Yuan Huang⁴, Weiwei Bi⁵, Huan-Feng Duan⁶, Dragan**
5 **Savic⁷ and Zoran Kapelan⁸**

6 ¹**Yiran Ji:** PhD student, College of Civil Engineering and Architecture, Zhejiang University, China.
7 yiranji@zju.edu.cn

8 ²**Feifei Zheng:** Professor, College of Civil Engineering and Architecture, Zhejiang University, China.
9 feifeizheng@zju.edu.cn. Corresponding author, Tel: +86-571-8820-6757. Postal address: A501, Anzhong
10 Building, Zijingang Campus, Zhejiang University, 866 Yuhangtang Rd, Hangzhou, 310058 China.

11 ³**Jiawen Du:** Master student, College of Civil Engineering and Architecture, Zhejiang University, China.
12 dujiawen@zju.edu.cn

13 ⁴**Yuan Huang:** Associate Professor, College of Water Conservancy & Hydropower Engineering, Hohai
14 University, Nanjing, China. huangyuan@hhu.edu.cn

15 ⁵**Weiwei Bi:** Lecturer, College of Civil Engineering, Zhejiang University of Technology, China.
16 weiweibi@zjut.edu.cn.

17 ⁶**Huan-Feng Duan:** Associate Professor, Department of Civil and Environmental Engineering, The Hong
18 Kong Polytechnic University, Hung Hom, Kowloon, 999077, Hong Kong. hf.duan@polyu.edu.hk.

19 ⁷**Dragan Savic:** Chief Executive Officer, KWR Water Research Institute, Dragan.Savic@kwrwater.nl;
20 Professor, Centre for Water Systems, University of Exeter, North Park Road, Exeter, EX4 4QF, United
21 Kingdom; Distinguished Professor, Universiti Kebangsaan Malaysia.

22 ⁸**Zoran Kapelan:** Professor, Delft University of Technology, Faculty of Civil Engineering and Geosciences,
23 Department of Water Management, Stevinweg 1, 2628 CN Delft, Netherlands. z.kapelan@tudelft.nl.

24
25

26 **Abstract:** Most of contamination source localization methods for water distribution systems (WDSs)
27 assumes the availability of accurate water quality models and multi-parameter online sensors, which
28 are often out of reach of many water utilities. To address this, a novel manual grab-sampling method
29 (MGSM) is developed to effectively and efficiently locate continuous contamination sources in a
30 WDS using a dynamic and cyclical sampling strategy. The grab samples are collected at a pre-
31 specified number of hydrants by the corresponding teams followed by laboratory tests. The MGSM
32 optimizes the sampling plan at each cycle by making the probability of contamination source(s) in
33 each sub-network as equal as possible, where sub-networks are determined by the selected hydrants
34 and current flow pipe directions. The CS's size is reduced at each cycle by exploiting sample testing
35 results obtained in the previous cycle until there are no further hydrants to sample from. Two real-
36 world WDSs are used to demonstrate the effectiveness of the proposed MGSM. The results obtained
37 show that the MGSM can significantly reduce the spatial range of the CS (to about 5% of the entire
38 WDS) for a range of scenarios including multiple contamination sources and pipe flow direction
39 changes. We found that an optimal number of sampling teams exists for a given WDS, representing
40 a balanced trade-off between detection efficiency and sampling/testing budgets. Due to its relative
41 simplicity the proposed MGSM can be used in engineering practice straightaway and it represents a
42 viable alternative to the methods associated with water quality models and sensors.

43 **Keywords:** Water distribution systems, manual grab-sampling method, contamination sources,
44 water quality

45

46 **1. Introduction**

47 A water distribution system (WDS) represents a basic lifeline infrastructure that closely relates to
48 the daily life and health safety of its served population (Qi et al., 2018). Typically, a WDS is spatially
49 distributed and thus inherently vulnerable to accidental and/or intentional contamination intrusion
50 (Ostfeld et al., 2014; Yang and Boccelli 2016; Zhang et al., 2020). For instance, over a five-day
51 period in October 2007, a boil-water notice was served on the majority of Oslo, Norway, as a result
52 of a combination of bacteriological, *Cryptosporidium* oocysts and *Giardia* cysts found in the samples
53 taken from the WDS (Robertson et al., 2008). More recently, on 26 July 2020, a contamination event
54 was reported in Hangzhou, China, where a sewer pipe was misconnected to a drinking water pipe in
55 a small suburb (ChinaNews, 2020). Unfortunately, these events were not detected by the water
56 quality warning systems of the local water utilities. The events were reported by the residents and/or
57 diagnosed by the hospitals. This implies that monitoring and protecting water quality safety are
58 still nontrivial challenges for many WDSs (Asheri Arnon et al. 2019).

59 To secure water quality safety in a WDS, extensive studies have been carried out to develop
60 contamination response systems (CRSs) (Giudicianni et al. 2020a). In principle, an effective CRS
61 should at least consist of a contamination warning and source identification (Rodriguez et al. 2021).
62 Regarding the contamination warning, a straightforward manner is to deploy online water quality
63 sensors within the WDS (Hart and Murray 2010). A warning is triggered once the concentration
64 of some particular water quality parameters (e.g., pH, turbidity) is above or below the sensor's
65 safety threshold. Ideally, placing a sensor at each possible location in the WDS can maximise the
66 capability to generate a warning when a contamination intrusion event occurs (Zheng et al. 2018).
67 However, it is difficult, if not impossible, to implement this approach due to the high capital and
68 maintenance costs associated with so many water quality sensors (Winter et al. 2019).

69 Consequently, many studies have focused on optimally deploying a limited number of water
70 quality sensors to maximize their detection/warning performance (Rathi and Gupta 2014). These
71 studies range from the use of different objective functions to identify appropriate water quality
72 sensor placement strategies (He et al. 2018; Naserizade et al. 2018), to the development of various
73 algorithms to enable effective optimization on this design problem (Hu et al. 2017). More recently,
74 efforts have been increasingly made to identify design solutions that provide a resilient water

75 quality sensor strategy. The approach does not only perform well when all sensors function
76 perfectly, but also can detect contamination events even under possible sensor failures (Ostfeld et
77 al., 2008; Zhang et al., 2020). Typically, the objective functions designed for the water quality
78 sensor placement problems are very complex as different aspects of contamination detection need
79 to be taken into account (e.g., detection likelihood, detection time delay, sensor reliability, different
80 consequences of non-detection, various uncertainties, Khorshidi et al. 2018). Studies have been
81 undertaken to develop various algorithms to effectively identify optimal water quality sensor
82 placement strategies based on these objective functions (Ung et al. 2017). Specifically, those
83 studies focus on developing either sophisticated search algorithms that enhance the design
84 solution's quality (Di Nardo et al. 2018; Hu et al. 2020) or advanced water quality modelling
85 approaches that improve the optimization efficiency (Naserizade et al. 2018; Ohar et al. 2015).

86 In parallel to the research progress on the early warning systems for contamination detection,
87 efforts have also been made to develop various algorithms for sourcing/localizing the
88 contamination injection locations according to the analysis of sensor data (Pries and Ostfeld, 2007).
89 These developments started by using the traditional optimization techniques, such as linear
90 programming (LP) scheme (Pries and Ostfeld, 2006). This was followed by the use of various
91 evolutionary algorithms (EAs) as they possess superior search capabilities compared to the
92 traditional LP and nonlinear programming (NLP) techniques (Pries and Ostfeld, 2008; Hu et al.,
93 2015; Li et al., 2021). While these algorithms have reliable performance in locating contamination
94 sources in hypothetical case studies, their practical application can be highly challenging. This is
95 mainly due to the "equifinality" issue associated with the identification of the source of the incident
96 (Jia et al., 2021a), where many different injection scenarios (contaminant concentration and
97 starting time) indicate a similar contamination impact. To address this issue, the Bayesian based
98 approaches have been proposed to identify contaminant sources, where the location with the
99 highest posterior probability is interpreted as the most plausible (Yang and Boccelli, 2014; Sankary
100 and Ostfeld, 2019; Jerez et al., 2021). More recently, machine learning algorithms have been
101 increasingly employed to facilitate contamination localization, such as the Random Forest
102 algorithm (Grbčić et al., 2020) and Convolutional Neural Network (Sun et al., 2019).

103 Detailed analysis of previous studies in terms of the CRS research shows that the majority of
104 contamination warning and source identification methods rely heavily on an accurate water quality

105 model (Vrachimis et al. 2020). This is one of the main reasons that may hinder their
106 implementation as a well-calibrated water quality model is usually not available for many water
107 utilities (Sankary and Ostfeld 2018). In addition, existing water quality modelling techniques are
108 still incapable of accurately reproducing contaminant reaction dynamics in WDSs, especially for
109 biochemical contaminants (Hart et al. 2019). While online sensors may provide reliable warning
110 information by measuring the contaminant concentration in real-time, they generally can only
111 measure a limited number of water quality parameters such as pH, turbidity, chlorine and
112 conductivity (Sun et al. 2019). Consequently, many other contaminants such as organics and
113 pathogenic microorganisms cannot be detected with certainty using online in-situ sensors. In
114 addition, water quality sensors are often expensive in both the purchase and maintenance,
115 especially for advanced sensors that are used to measure complex substances (He et al., 2018).
116 Therefore, the water quality sensors are often sparsely distributed in many WDSs (Ostfeld et al.,
117 2014).

118 The contamination events within the WDS can be classified into three different types, which are
119 intentional events (Type 1), accidental events (Type 2) and events caused by the WDS itself (Type
120 3). For Type 1, the contamination can be toxic substances that are intentionally injected into the
121 WDS, typically during a short time period. Such events can result in serious consequences and hence
122 need a quick response at all costs (Ostfeld et al., 2014). Type 2 is often represented by the
123 misconnections between water supply pipes and greywater /sewer pipes that have been reported in
124 China (He et al., 2018). Type 3 can be caused by structural damages to pipes (e.g., contamination
125 due to pipe corrosion or leaks, Zhang et al., 2020) or biochemical substances (e.g., microorganisms)
126 activated by the water at a particular level of turbulence (He et al., 2019).

127 Typically, within Types 2 and 3, the contamination exists *continually* in the WDS until the source(s)
128 is localized and eliminated. These contamination substances (e.g., metal, microorganism, organic)
129 often have the following properties: (i) they can be colorless and tasteless, and hence cannot be
130 directly detected by tap-water users; (ii) they do not induce quick, serious public health consequences
131 (i.e., this study focuses on the contamination events with chronic but no acute health effects) and
132 hence their source(s) localization needs to be conducted without interrupting water supply; and (iii)
133 they may not be directly detected by online water quality sensors as the majority sensors typically
134 monitor simple quality parameters such as chlorine, pH, turbidity and conductivity. These properties

135 motivate the development of the proposed manual grab-sampling method (MGSM) to efficiently
136 and effectively identify continuous contamination sources of Types 2 and 3 in WDSs.

137 The proposed MGSM is an iterative manual grab-sampling method (MGSM) to enable effective
138 contaminant detection and localization. This is followed by gathering comprehensive water quality
139 parameter information with the aid of laboratory tests. The MGSM is particularly useful for the
140 cases that the online quality sensors are sparsely distributed (or completely unavailable) or sensors
141 cannot measure the contaminants (Wong et al., 2010). The MGSM does not need water quality
142 modelling and can identify the contamination location without encountering the “equifinality”
143 issue. In addition, for the cases that the labour is plentiful with low cost, the MGSM is preferred
144 as it provides the spatial distribution of water quality measurements at a reduced cost when
145 compared to fixed sensors (Mann et al., 2012). Therefore, manual grab-sampling can be an
146 important strategy for water utilities interested in water quality safety in the WDS, which can
147 supplement the information obtained from existing online sensors.

148 Despite the merits and practical significance of the MGSM for the cases with sparsely distributed
149 sensors and relatively low labor costs, relevant research on this topic is surprisingly rare. Amongst
150 few relevant studies, one significant example is from the work of Wong et al. (2010), where a
151 Mixed-Integer Linear Programming formulation is proposed to determine optimal locations for
152 manual grab sampling after a contamination event is detected in a WDS. In their study, the optimal
153 manual grab sample locations are identified by maximizing the total pair-wise distinguishability
154 of candidate contamination events (eliminate unlikely events as much as possible). While Wong
155 et al. (2010) showed that a contamination event can be identified by their proposed method with
156 significantly improved efficiency, its success was conditioned on a few critical assumptions. These
157 assumptions include: (i) each node in the WDS has an equal probability of being the source of
158 contamination intrusion, (ii) only one contamination event can occur in the WDS, and (iii) the pipe
159 flow direction cannot change during the entire sampling process. However, these assumptions can
160 significantly violate the real conditions as the contamination intrusion can occur at any pipe
161 location and a long pipe is typically associated with a higher contamination probability (He et al.,
162 2018). Furthermore, although the probability of simultaneous multiple contamination intrusions is
163 low, their occurrence is still possible in large WDSs (Butera et al., 2021). In addition, flow

164 direction changes are likely to occur in some pipes in a large WDS with multiple supply sources
165 (Qi et al., 2018).

166 The main contribution of this paper is the proposal of an improved water quality MGSM for
167 detecting and localizing continuous contamination sources in WDSs. The newly developed method
168 employs a dynamic and cyclical sampling strategy based on the hydrant locations in a WDS. The
169 novel aspect of the proposed method is the simple and effective way developed to split the network
170 after each round of sampling, thereby significantly enhancing the efficiency of the entire detection
171 process. In addition, the proposed method is novel in that the optimal sampling locations are
172 determined by making the probability of contamination source in each sub-network based on the
173 current flow pipe directions as equal as possible at each cycle. The results of these samples are
174 subsequently analyzed and employed to drive the sampling strategy for the next cycle. It is
175 highlighted that the proposed MGSM is an alternative to these literature methods (sensor-based
176 methods) in the cases where: (a) sensors are sparsely distributed or not available (e.g. lack of
177 existence of suitable sensors), (b) the low-cost labour force is available, and (c) the contamination
178 events have slow or low impacts to the water quality in the WDSs.

179 **2. Methods**

180 The basic premise of the proposed MGSM is: (1) select a given number of sampling points (hydrants
181 of the WDS) in the studied area based on the testing capacity of the laboratory (i.e., the number of
182 samples that can be tested simultaneously) and the number of sampling teams, with all pipes within
183 the candidate area considered as possible contamination sources, (2) narrow down the range of the
184 candidate areas containing contamination source(s) based on sample testing results, and (3) repeat
185 steps (1) and (2) until the range of candidate areas with contamination source(s) cannot be further
186 narrowed down. The key to effectively implementing this new MGSM is how to automatically select
187 the appropriate hydrants in each cycle of the above methodology to reduce the total number of cycles,
188 thereby quickly localizing the pollution source(s) in the WDS. It is noted that every length of pipe
189 between two hydrants within the WDS is considered as the contamination source. Therefore, the
190 proposed MGSM can account for both the scenarios that the contamination sources are in pipes or
191 junctions. While the proposed MGSM is demonstrated using hydrants in this study, any other

192 sampling facilities (e.g., taps) can be easily handled by simply treating them as hydrants within the
193 algorithm implementation.

194 Section 2 presents the details of the proposed MGSM, including the associated theoretical
195 foundations (e.g., the development of the objective function), the MGSM algorithm structure, the
196 illustration of the proposed MGSM and the optimization method to implement the MGSM.

197 **2.1 Theoretical foundations for the proposed MGSM**

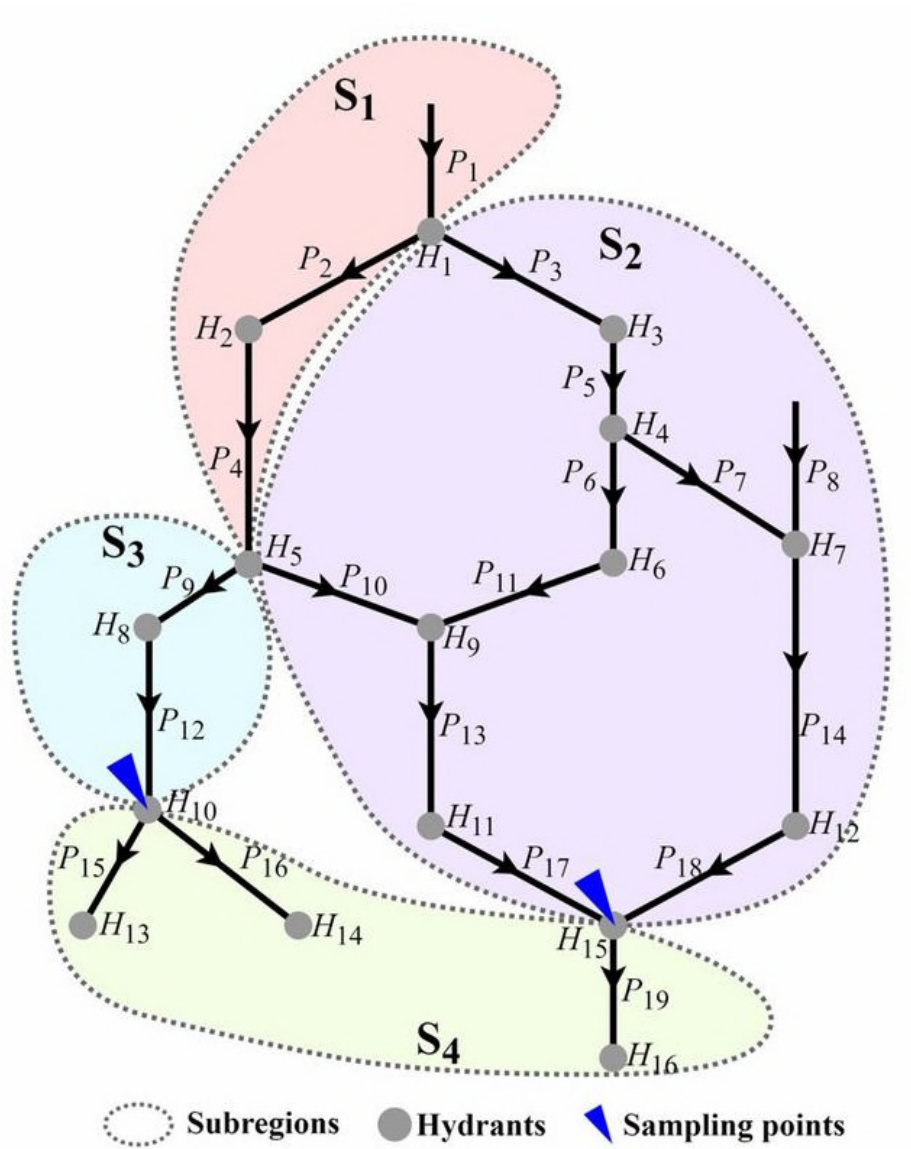
198 Section 2.1 introduces the theoretical foundations of the proposed MGSM, including the proposal of
199 a method to enable the WDS partitioning and the development of the objective function of the
200 proposed MGSM. The details are given below.

201 **2.1.1 WDS partitioning based on sampling locations and flow directions**

202 As previously stated, the proposed MGSM attempts to identify the optimal sampling locations
203 (hydrants) at each cycle, aimed to minimize the total number of cycles (equivalent to the efficiency
204 and cost of the entire process). Within the MGSM, the entire WDS is partitioned into different sub-
205 networks based on sampling locations and flow directions at a given point in time. Specifically, if a
206 hydrant H in the system is selected as the sampling point, all pipes in the WDS can be divided into
207 two sub-networks: all upstream pipes relative to the selected hydrant H , denoted as \mathbf{U}_H , and
208 remaining pipes whose flows do not go through H , denoted as \mathbf{N}_H . If two hydrants (H_1 and H_2) are
209 selected as the sampling points, four sub-networks can be identified, respectively representing the
210 common group of pipes upstream of both selected hydrants ($\mathbf{U}_1 \cap \mathbf{U}_2$), the unique group upstream of
211 one hydrant only ($\mathbf{U}_1 \cap \mathbf{N}_2$ and $\mathbf{U}_2 \cap \mathbf{N}_1$), and not the upstream of both hydrants ($\mathbf{N}_1 \cap \mathbf{N}_2$). Using this
212 process, for a number of n sampling points in a WDS, e.g., $\{H_1, H_2, \dots, H_n\}$, a total of $T=2^n$ sub-
213 networks, $\{\mathbf{S}_1, \mathbf{S}_2, \dots, \mathbf{S}_T\}$, can be obtained theoretically.

214 Figure 1 illustrates how the proposed MGSM identifies the WDS sub-networks based on two
215 sampling locations. A total of 16 hydrants are available that can be considered as the potential
216 sampling points, where the arrows represent pipe flow directions. For illustration, hydrants 10 (H_{10})
217 and 15 (H_{15}) are selected as sampling points to enable network partitioning. Four different sub-
218 networks are identified using the proposed MGSM, which are $\mathbf{S}_1=\{P_1, P_2, P_4\}$, $\mathbf{S}_2=\{P_3, P_5, P_6, P_7,$
219 $P_8, P_{10}, P_{11}, P_{13}, P_{14}, P_{17}, P_{18}\}$, $\mathbf{S}_3=\{P_9, P_{12}\}$, $\mathbf{S}_4=\{P_{15}, P_{16}, P_{19}\}$. It can be observed that pipes in \mathbf{S}_1

220 are in the common upstream group for H_{10} and H_{15} and flows for pipes in S_4 do not go through any
 221 of the two hydrants. Pipes in S_2 are those that are upstream of H_{15} but not H_{10} , and Pipes in S_3 are
 222 upstream of H_{10} but not H_{15} .



223

224 **Figure 1: Illustration of the WDS sub-networks identified by the proposed MGSM based**
 225 **on two sampling locations, with arrows representing pipe flow directions**

226 For the n sampling points $\mathbf{A}=\{H_1, H_2, \dots, H_n\}$, the outcome of the test at each sampling point is
 227 either that the sample is contaminated or non-contaminated. Therefore, there are 2^n possible results
 228 for n sampling points, in which each contaminated outcome corresponds to the contamination source

229 being located in a certain sub-network or many sub-networks when contaminations are found in
 230 many sampling locations. For example, if the contamination is detected at both H_{10} and H_{15} , as in
 231 Figure 1, it can be derived that the contamination source(s) may be located in the common upstream
 232 group of pipes (\mathbf{S}_1 in Figure 1). The source can also be in the two sub-networks (\mathbf{S}_2 and \mathbf{S}_3) upstream
 233 of one of the two sampling locations. When only one sampling point indicates contamination, it can
 234 be determined that the source is located in the area upstream of the sampling point where
 235 contamination is detected, that is, \mathbf{S}_2 or \mathbf{S}_3 . When results show no contamination at both sampling
 236 points, then the contamination source(s) is located in an area outside all the upstream parts of the
 237 two sampling points, that is, \mathbf{S}_4 in Figure 1. This is the basic localization principle used in the
 238 proposed MGSM in this study.

239 Once a sub-network or a few sub-networks are selected as potential contamination sources based on
 240 the sample testing results, all pipes in this/these sub-network(s) are considered as candidates. This is
 241 followed by the further use of the partitioning method to narrow down the spatial range to localize
 242 the source. In other words, the network partitioning needs to be carried out at each cycle of the entire
 243 sampling process based on the updated candidate pipes with potential contamination sources.

244 **2.1.2 The development of the objective function of the proposed MGSM**

245 Conditioned on the identified T sub-networks, the mathematical expectation ($E(\mathbf{A})$) of a given set of
 246 sampling points (\mathbf{A}) in localizing the location of the contamination source can be expressed as

$$E(\mathbf{A}) = \sum_{i=1}^T p_i \cdot L_i \quad (1)$$

247 where p_i is the probability of the i^{th} sub-network that have the contamination source, and L_i is the
 248 corresponding total pipe length of this sub-network. Since the proposed MGSM mainly aims to
 249 detect contamination types 2 and 3 (see section 2 for details), the probability of a contamination
 250 source being located on each unit length of pipe can be considered identical. This results in the
 251 probability of contamination source being in any sub-network i equal to the ratio of the pipe length
 252 of the sub-network L_i to the total pipe length L_{all} in the entire WDS. Mathematically, it gives,

$$E(\mathbf{A}) = \sum_{i=1}^T \frac{L_i}{L_{all}} \cdot L_i = \frac{1}{L_{all}} \sum_{i=1}^T L_i^2 \quad (2)$$

253 Thus, the objective function for calculating the optimal sampling group can be expressed as follows:

$$\text{Minimize: } F(\mathbf{A}) = \frac{E(\mathbf{A})}{L_{all}} = \frac{1}{L_{all}^2} \sum_{i=1}^T L_i^2 \quad (3)$$

254 where $F(\mathbf{A})$ is a dimensionless number by dividing $E(\mathbf{A})$ using L_{all} , representing the ratio of candidate
255 area with contamination source identified by the sampling group relative to the total pipe length of
256 the entire WDS being considered. \mathbf{A} is the decision variables, representing the hydrant sampling
257 strategy. The minimization of $F(\mathbf{A})$ physically indicates a minimum pipe length of the sub-network
258 with contamination source(s) to be identified by the selected sampling points.

259 Cauchy–Schwarz Inequality (Bhatia and Davis, 1995) can be used to further explain the
260 minimization of Equation (3), which is

$$T \times (L_1^2 + L_2^2 + \dots + L_T^2) \geq (L_1 + L_2 + \dots + L_T)^2 \quad (4)$$

$$\text{Namely } F(\mathbf{A}) = \frac{1}{L_{all}^2} \sum_{i=1}^T L_i^2 \geq \frac{1}{T} \quad (5)$$

261 For $L_1=L_2, \dots, =L_T$, the equation holds. Under this condition, when only one hydrant is selected as the
262 sampling point in each cycle, the optimal hydrant divides the WDS into two sub-networks such the
263 pipe length of its upstream section is half of the total length. When n hydrants are selected as the
264 sampling points in each cycle, theoretically, the optimal hydrant group bisects the WDS to 2^n sub-
265 networks with identical pipe lengths across different sub-networks. In other words, the minimization
266 of Equation (3) (i.e., $L_1=L_2, \dots, =L_T$) can be interpreted as using a specified number of sampling points
267 to assign the pipes into T sub-networks with the minimum difference in pipe length at each cycle.
268 This is equivalent to the bi-section approach in computer science, and hence it is expected that such
269 a method can achieve a statistically efficient sampling strategy to localize the contamination source.
270 It is noted that the proposed optimization method may not be able to guarantee global optimality, but
271 it can offer a near-optimal solution that can be efficiency found at each cycle.

272 The pipe length is used to split the WDS in this study due to its simplicity and efficiency. However,
273 a more refined method may need to account for water velocities or flow volumes, both of which can
274 be correlated with pipe diameters, as well as can account for the amounts of contaminants moving

275 through the pipes. Therefore, partitioning the WDS with the aid of both pipe length and water
276 velocity can be an important future research focus.

277 2.2 The algorithm of the proposed MGSM

278 The implementation of the proposed MSGM can be triggered by (i) the routine water quality
279 checking operation required by the water utilities, (ii) abnormal signals from online water quality
280 sensors (e.g., chlorine sensors) that are often installed at the outlets of the districted metering areas
281 (DMAs), or (iii) positive testing results of samples at the outlets of the DMAs or at the important
282 locations within the WDS area. Figure 2 shows the algorithm details of the proposed MGSM in
283 localizing contamination source(s). As shown in this figure, when the number of sampling locations
284 at each cycle is $n=1$, the sampling hydrant is selected by minimizing Equation (3), where the
285 minimization method is elaborated in Section 2.4. The candidate sub-network (**CS**) that may contain
286 contamination source(s) is updated at each cycle based on the sample testing results (Case A1 and
287 Case A2 in Figure 2). If n is greater than 1, the algorithm of the proposed MGSM becomes more
288 complex, with details given in Figure 2. At the beginning (i.e., flag=0, and the MGSM is triggered),
289 the n optimal sampling locations are identified by minimizing Equation (3) for the entire WDS being
290 considered (i.e., **CS** is the entire WDS). This is followed by the application of selection strategy 1
291 (SA1) to update the **CS** for the next cycle, where three different cases (Case B1, B2 and B3) can be
292 available. For Case B2 (only one sample hydrant has contamination) and B3 (all sample hydrants
293 are contamination free), it is straightforward to select the **CS** for the next cycle as shown in Figure
294 2.

```
Specify the number of sampling points  $n$   
Set the cycle  $c=1$ , flag=0, the candidate sub-network (CS) as the entire WDS  
While True  
{  
  If  $n = 1$   
  {  
    Select  $n$  sampling hydrant for the CS by minimizing Equation (3)  
    Update the CS according to sample testing results  
    Case A1: the sample is contaminated  
      Select the sub-network (US) upstream of the selected hydrant  
    Case A2: the sample is contamination free  
      Select the sub-network that is not the upstream of the selected hydrant  
     $c = c + 1$   
  }  
  Else  
  {  
    If flag=0
```

```

{
  Select  $n$  sampling hydrants for the CS by minimizing Equation (3)
  Update the CS according to sample testing results using Selection strategy 1 (SA1):
  Case B1: more than one hydrant sample are contaminated
    Select the common sub-network (CUS) upstream of the contaminated hydrants
    Set flag=1
  Case B2: only one hydrant sample is contaminated
    Select the unique sub-network upstream of the contaminated hydrant
  Case B3: no hydrant samples are contaminated
    Select the sub-network that is not the upstream of the selected hydrant
   $c = c + 1$ 
}
If flag=1
{
  If the CUS exists and its most downstream hydrant is not sampled
  Assign one sample point at the most downstream hydrant of the CUS
  Select  $n-1$  sampling hydrants for the CS by minimizing Equation (3)
  Update the CS(s) according to testing results at the end hydrant
  If the end hydrant is contaminated
    Select the CS using the SA1 mentioned above
  Else
    Selection strategy 2 (SA2):
    Select the CS(s) as the union of USs of the hydrants showing evidence of
    contamination minus the union of USs of contamination-free hydrants and the CUS
     $c = c + 1$ 
  Else If the CUS does not exist
    Select the CS(s) using the SA2 mentioned above
  Set flag=0
}
}
If no hydrant can be sampled in the selected sub-network
  break
}

```

295

Figure 2: The algorithm of the proposed MGSM

296 When more than one sample hydrant is contaminated (Case B1), the common upstream sub-network
297 (**CUS**, which is theoretically available) is selected as the **CS** for the next cycle ($c=c+1$). If this **CUS**
298 exists and its most downstream hydrant is not sampled, one sampling location is assigned to this
299 hydrant. The remaining $n-1$ sampling locations are determined by minimizing Equation (3). The **CS**,
300 which is temporally considered as the **CUS**, is now updated using the following method based on
301 test results of the most downstream hydrant. If that hydrant is contaminated, the **SA1** is employed to
302 update the **CS**, otherwise, the **SA2** (see Figure 2) is used to update the **CS**. Specifically, the **SA2**
303 selects the **CS(s)** as the union of all upstream sub-networks (**USs**) of hydrants where contamination

304 was detected, minus the union of USs of contamination-free hydrants and the CUS. Note that if the
305 selected CUS does not exist in the WDS, the SA2 is used to update the CS(s).

306 The proposed MGSM in Figure 2 can handle both the single and multiple contamination sources in
307 a DMA of a WDS. However, each MGSM run identifies only a sub-network that contains a
308 contamination source of the smallest spatial extent. This identified region may need to be blocked
309 for engineering operations (e.g., disconnect the misconnections, repair the leaks, or replace the pipes),
310 to remove the contamination source(s). Sampling tests with a few contaminated hydrants may
311 indicate the presence of multiple contamination sources in different WDS regions. For such cases,
312 once the identified contamination source(s) is fixed, the proposed MGSM can be applied to the
313 potential CSs (instead of the entire WDS) derived by the sampling test results combined with
314 knowledge of pipe flow directions. Such a CS selection can be easily performed by engineering
315 experience, but it is difficult to be shown by formal procedures. However, it is also straightforward
316 to simply apply the MGSM to the entire WDS to identify the other contamination source(s), after
317 the already localized source(s) are fixed.

318 The methodology assumes that all hydrants selected in one cycle can be sampled at the same flow
319 direction status. This assumption is practically reasonable as the time required to grab samples is
320 often short and the frequency of flow direction change is typically low (e.g., once a day, Wong et
321 al., 2010). While flow direction changes may exist within the supply boundary of some real large
322 WDSs, its associated region is often rather small. Therefore, the change of the flow directions will
323 not significantly affect the application of the proposed MGSM. If the WDS region with changing
324 flow direction is large and known, it can be easily accounted for by the proposed MGSM based on
325 an important assumption. This assumption is that the time between the start of the flow direction
326 change and the next sampling cycle is significantly greater than the longest travel time from the
327 source to the sample locations. In other words, the contaminant distribution has to be consistent with
328 the current flow regime and can have no residual effects from the previous flow regime. Based on
329 this assumption, the flow direction changes can be considered by the WDS partitioning process as
330 described in Section 3.1.1, which would accordingly affect the formulation of sub-networks and
331 hence the identification of the optimal sampling locations (Equation 3).

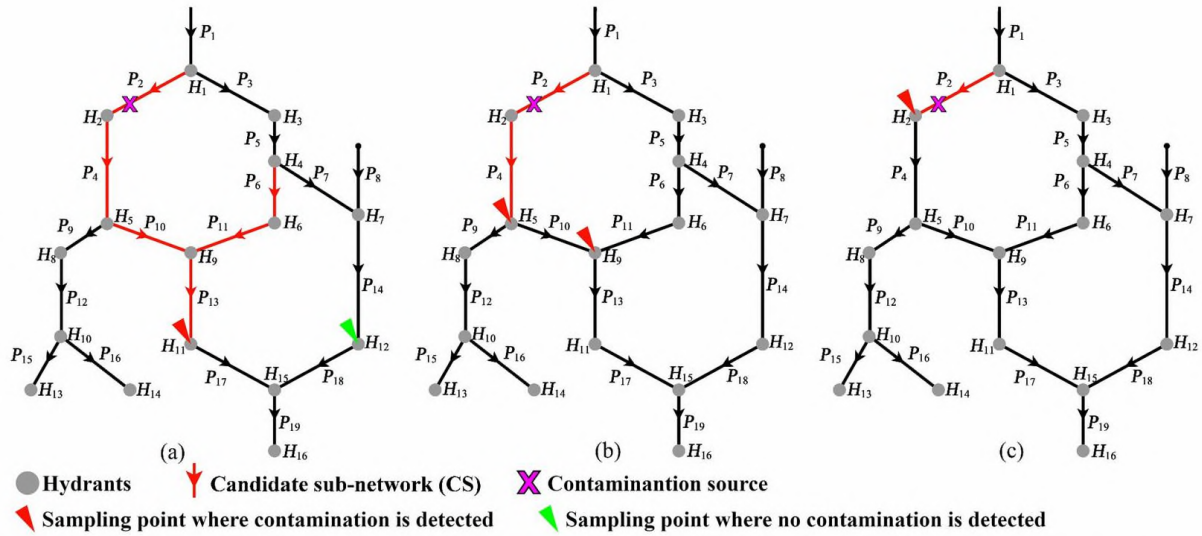
332 **2.3 Illustration of the proposed MGSM**

333 The proposed MGSM is illustrated with two scenarios, including the single contamination source
334 and the two contamination sources simultaneously exist in the WDS, with details given below.

335 **2.3.1 Single contamination source**

336 We first illustrate the application of the proposed MGSM (Figure 2) using a single contaminating
337 source as shown in Figure 3. The single contamination source is in P_2 , and two sampling locations
338 ($n=2$) are identified at each cycle. At the first cycle, the entire WDS is set as a candidate sub-network
339 (**CS**), and a total of 120 sampling combinations (two out of 16 total hydrants) are possible. The
340 mathematical expectations (Equation 3) corresponding to these 120 combinations are calculated by
341 enumeration and the combination with the minimum $F(\mathbf{A})$ value is selected. Consequently, two
342 hydrants $\{H_{11}, H_{12}\}$ are identified as the sampling points yielding the lowest objective function value
343 (Equation 3), as shown in Figure 3(a). Based on the assumed location for the contamination source,
344 the sample from hydrant H_{11} is contaminated while the sample from H_{12} is not based on the
345 laboratory tests. Therefore, the **CS** is updated to be a unique sub-network upstream of H_{11} (and not
346 pipes upstream of H_{12}) based on Case B2 in Figure 2, that is, the red pipes shown in Figure 3(a).

347 In the second cycle of sampling, the mathematical expectations corresponding to different hydrant
348 groups are calculated according to the updated **CS** determined in the previous cycle. The resultant
349 optimal strategy is the combination of H_5 and H_9 as it produces the lowest objective function value.
350 Testing results on these two hydrant samples show that both are contaminated, indicating that the
351 contamination source exists in the common upstream sub-network (**CUS**) of H_5 and H_9 . Therefore,
352 the **CS** is updated as the **CUS** based on Case B1 (Figure 2), which is $\{P_2, P_4\}$ as represented by red
353 lines in Figure 3(b). In the third cycle of sampling, there is only one hydrant location, H_2 , so the
354 contamination source is successfully detected on P_2 , which is the exact location of the contamination
355 source.



356

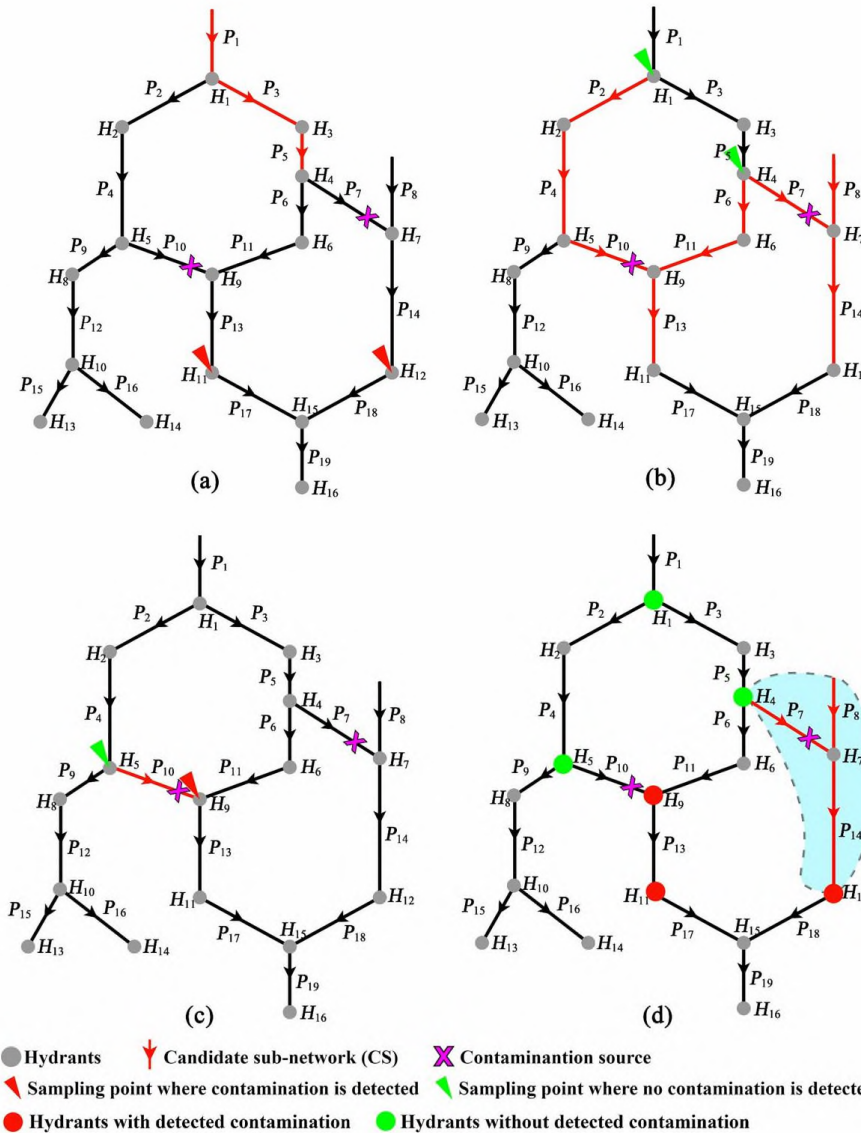
357 **Figure 3: Source localization process for the contamination at P_2 : (a) the first cycle ($c=1$) of**
 358 **sampling and testing; (b) sampling and testing at $c=2$; (c) sampling and testing at $c=3$**

359 **2.3.2 Two contamination sources**

360 Figure 4 illustrate the application of the proposed MGSM (Figure 2) in dealing with two
 361 contamination sources. In this figure, the contamination sources are in P_7 and P_{10} , and two sampling
 362 locations ($n=2$) are identified at each cycle. As the same with the single contamination source in
 363 Figure 3(a), the hydrants H_{11} and H_{12} are selected as the sampling points at the first cycle by
 364 minimizing Equation (3) (the enumeration method is used for this small WDS). The testing results
 365 show both hydrants are contaminated, and accordingly, the CS is updated to be the common
 366 upstream sub-network (CUS, red pipes in Figure 4(a)) using Case B1 in Figure 2. Since the CUS
 367 exists and its most downstream hydrant (H_4) is not sampled, H_4 is selected as one sampling location
 368 and the other location (H_1) is identified with the aid of Equation (3) in the second cycle ($c=2$).

369 Based on the locations of the two contamination sources, the end hydrant H_4 should show no
 370 contamination in the laboratory test and selection strategy 2 (SA2) is used to update the CS. More
 371 specifically, for such cases, the CS can be described as UA-UB-CUS (CUS = { P_1, P_3, P_5 }), where
 372 UA is the union of sub-networks (USs) upstream of contaminated hydrants (i.e., H_{11} and H_{12} at $c=1$)
 373 and UB is the union of USs sampling hydrants without contaminations (it is null at $c=1$). This is
 374 followed by the application of the proposed method at $c=3$, where two hydrants (H_5 and H_9) are
 375 selected as the sampling points. The resultant CS is P_{10} using Case B2 in Figure 2 based on test

376 results (H_5 is not contaminated, but H_9 is), which is the unique upstream sub-network of H_9 . Since
 377 no hydrants can be sampled in the current CS (i.e., P_{10}), P_{10} is successfully identified with the
 378 contamination source. The run of the proposed MGSM (Figure 2) is finalized.



379
 380 **Figure 4: Source localization process for two contamination cases at P_7 and P_{10} : (a) the first**
 381 **cycle ($c=1$) of sampling and testing; (b) sampling and testing at $c=2$; (c) sampling and**
 382 **testing at $c=3$; (d) the CS identified (shaded pipes) for the next MGSM run, where the red**
 383 **and green dots represent test results of the previous MGSM run**

384 To identify the second contamination source in P_7 , the s localized source in P_{10} needs to be fixed
 385 before the implementation of the next MGSM run. This is because the proposed MGSM identifies

386 only one contamination source for each run. Prior to the application of the next MGSM run, the
387 identified contamination source(s) need to be eliminated. In addition, all the test results of hydrant
388 samples and pipe flow direction information can be jointly used to derive the potential CS for the
389 next MGSM run. For the given example, the CS can be identified as the red pipes in Figure 4 (d)
390 based on the test results of the previous MGSM run (red and green dots) since (i) the test on H_4
391 shows no contamination but H_{12} does, and (ii) the identified source at P_{10} is not upstream of H_{12} .
392 This CS is only a small proportion of the entire WDS, thereby greatly improving the efficiency of
393 the next MGSM run. However, for cases when the CS cannot be determined by the existing
394 information provided by sample test results and pipe flow directions, the entire WDS (after the
395 identified contamination source(s) is eliminated) is considered as the CS again to enable the
396 application of the proposed MGSM.

397 In this subsection, one and two contamination sources are used to illustrate the proposed MGSM due
398 to the high likelihood of those events occurring in real WDS. In addition, two sampling locations are
399 used at each cycle for illustration purposes, where the pipe flow directions are not changed. However,
400 the application procedures with details given in Figure 2 are generic, and hence can be applied to
401 other scenarios such as different number of sampling locations, different contamination sources and
402 the WDS with possible pipe flow changes (further explanation of which is given in Section 4)

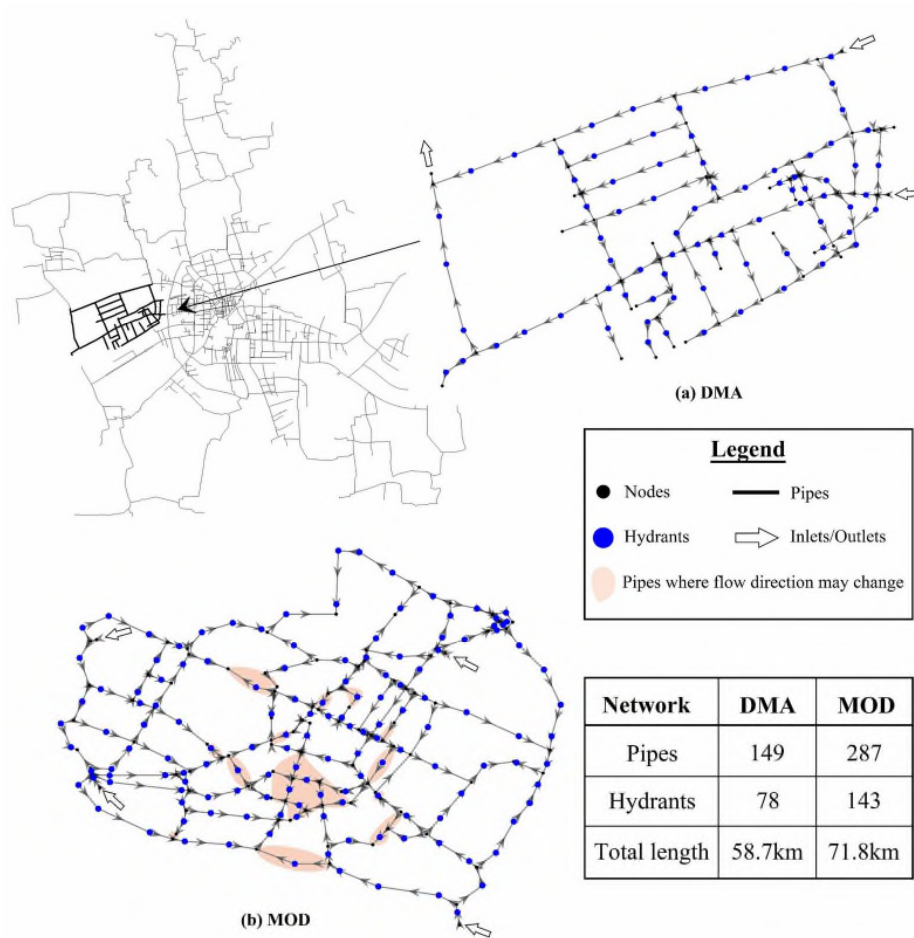
403 **2.4 Optimization method to minimize the objective function**

404 As shown in Figure 2, the proposed MGSM algorithm requires an optimization method to minimize
405 the objective function (Equation 3). While the enumeration method can be effective when dealing
406 with small WDSs and with a low number of sampling locations at each cycle, it is computationally
407 intractable for real and large WDSs. More specifically, for a case with n sampling points applied to
408 a WDS with a total of N hydrants, the number of all possible combinations is C_N^M . This value
409 increases exponentially with n and N becoming larger, leading to a rapid increase in computing time
410 and deterioration of detection effectiveness.

411 To solve the computational issue, the Monte Carlo (MC) method is used in this study as an alternative
412 to the enumeration approach in the process of determining the optimal sampling group to improve
413 detection efficiency for large-scale WDSs. The selection of the MC method is mainly due to its

414 simplicity and reasonable performance in offering near-optimal solutions (Maier et al., 2014). This
 415 is practically meaningful as in many engineering cases providing near-optimal solutions within a
 416 given time framework are more important than identifying global optimums with large
 417 computational overheads (Maier et al., 2014). Nevertheless, an advanced optimization algorithm can
 418 be developed for the proposed MGSM in future, which is not the focus of the present paper.

419 **3. Case studies**



420
 421 **Figure 5: (a) the DMA case study and (b) the MOD case study, where arrows indicate flow**
 422 **directions**

423 Two distribution networks (Figure 5) are used to demonstrate the utility of the proposed MGSM.
 424 Specifically, the DMA (district meter area) case study is a part of a real-world WDS in China (Figure
 425 5a) that consists of 149 pipes (58.7 km in length) and 78 fire hydrants. It has two inlets and one outlet,

426 and the flow direction in this network (shown in Figure 5(a)) does not change. The MOD pipe
427 network is a benchmark WDS of the city of Modena in Italy (Bragalli et al., 2012). This network
428 consists of 4 reservoirs (sources), 287 pipes (71.8 km in length) and 143 fire hydrants. Due to the
429 water level changes in the four reservoirs and variations in residential water consumption, the flow
430 directions of some pipes (shaded pipes in Figure 5(b)) in the MOD network change over time.

431 While the demonstration of the proposed MGSM using a very large WDS is academically necessary,
432 but in practice the MGSM is mainly used for a DMA or a region of the entire WDS. This is because
433 (i) many WDSs have been managed by DMAs, which can greatly enhance the operation efficiency,
434 and (ii) for the WDSs with no DMAs, water quality safety checking or contamination sourcing is
435 likely to be conducted region by region. It is highly unlikely to simultaneously consider all the pipes
436 of the entire large network as the contamination sources. Therefore, we demonstrate the proposed
437 method using two case studies at a DMA scale level.

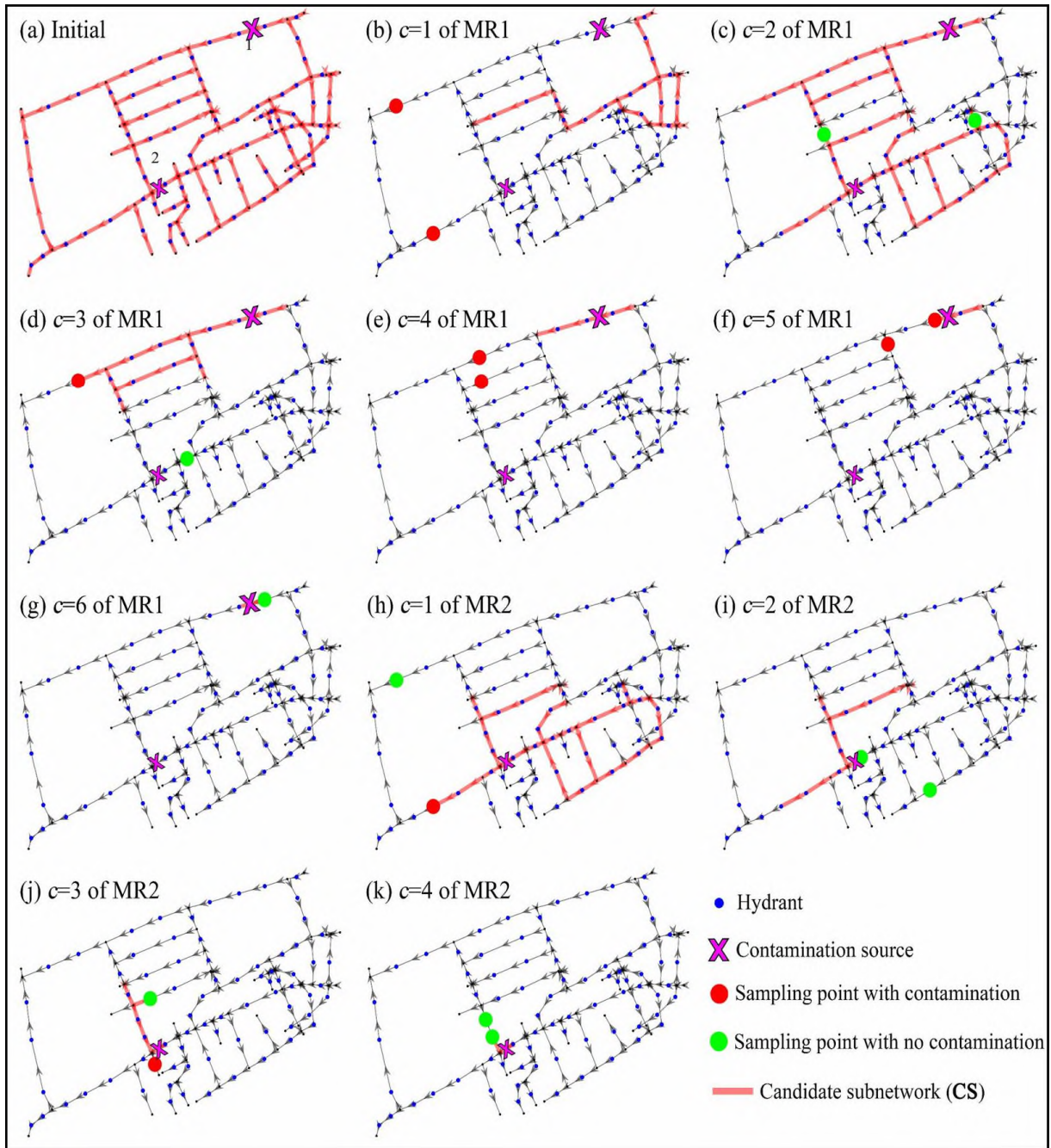
438 For both case studies, we have analyzed a series of different combinations of sampling locations (i.e.,
439 the number of hydrants that can be simultaneously sampled) at each cycle, with n ranging from 2
440 to 10. The number of potential contamination sources varies from one to three for these two WDSs.
441 The size of the MC method is determined to be 10,000 based on a preliminary analysis for both case
442 studies, but a larger value may be required for larger WDSs. The proposed MGSM is coded in C++
443 computing language with the aid of EPANET2.0 as the hydraulic solver to identify pipe flow
444 directions (He et al., 2018). For the DMA case study with 78 hydrants and two contamination sources,
445 the proposed method was tested using two and 10 potential sampling locations at each cycle required
446 an average of 102 and 54 seconds, respectively, on a PC with Intel i5-9400F CPU@2.90GHz. For
447 the MOD network with 143 hydrants and two contamination sources, the proposed MGSM with two
448 and 10 sampling locations at each cycle needs an average of 212 and 92 seconds, respectively. This
449 implies that the proposed method is very efficient to identify the optimal sampling locations based
450 on the test results. To enable the statistically rigorous analysis, for the single contamination source,
451 we considered all possible scenarios with one source assigned to each pipe of the network. For two
452 and three contamination sources, a total of 100 different randomly generated scenarios are
453 considered.

454 **4. Results and Discussion**

455 The proposed MGSM is demonstrated using the effectiveness (Section 4.1), the efficiency (Section
456 4.2) and the cost (Section 4.3) as shown in Section 4. The effectiveness is measured by the length of
457 finally identified pipes relative to the total pipe length of the entire WDS. The efficiency is measured
458 by the total number of sampling cycles, and the cost associated with the sampling process is
459 measured by the total number of samples that need to be tested in laboratory.

460 **4.1 Effectiveness of the proposed MGSM**

461 Figure 6 illustrates the application procedures of the proposed MGSM in dealing with the DMA case
462 study with two contamination sources (1 and 2 in Figure 6a) and two sampling locations at each
463 cycle. Two different MGSM runs (MR1 and MR2) are performed for this scenario, where the second
464 run assumed that the contamination source identified in the first run was eliminated. As shown in
465 this figure, in the beginning, the entire DMA is considered as the candidate sub-network (**CS**, Figure
466 6(a)) assuming that the water sample test at the outlet of this DMA shows contamination. This is
467 followed by the application of the MGSM, where six and four cycles were carried out to localize
468 contamination sources 1 and 2, respectively. The final identified pipe lengths associated with
469 contamination sources 1 and 2 are 741 and 762 meters, which represent only 1.26% and 1.30% of
470 the entire DMA, respectively. This implies that the proposed MGSM is able to effectively narrow
471 down the spatial range of pipes that contain contamination sources, which can greatly facilitate the
472 subsequent field investigations to eliminate the cause of the problem.

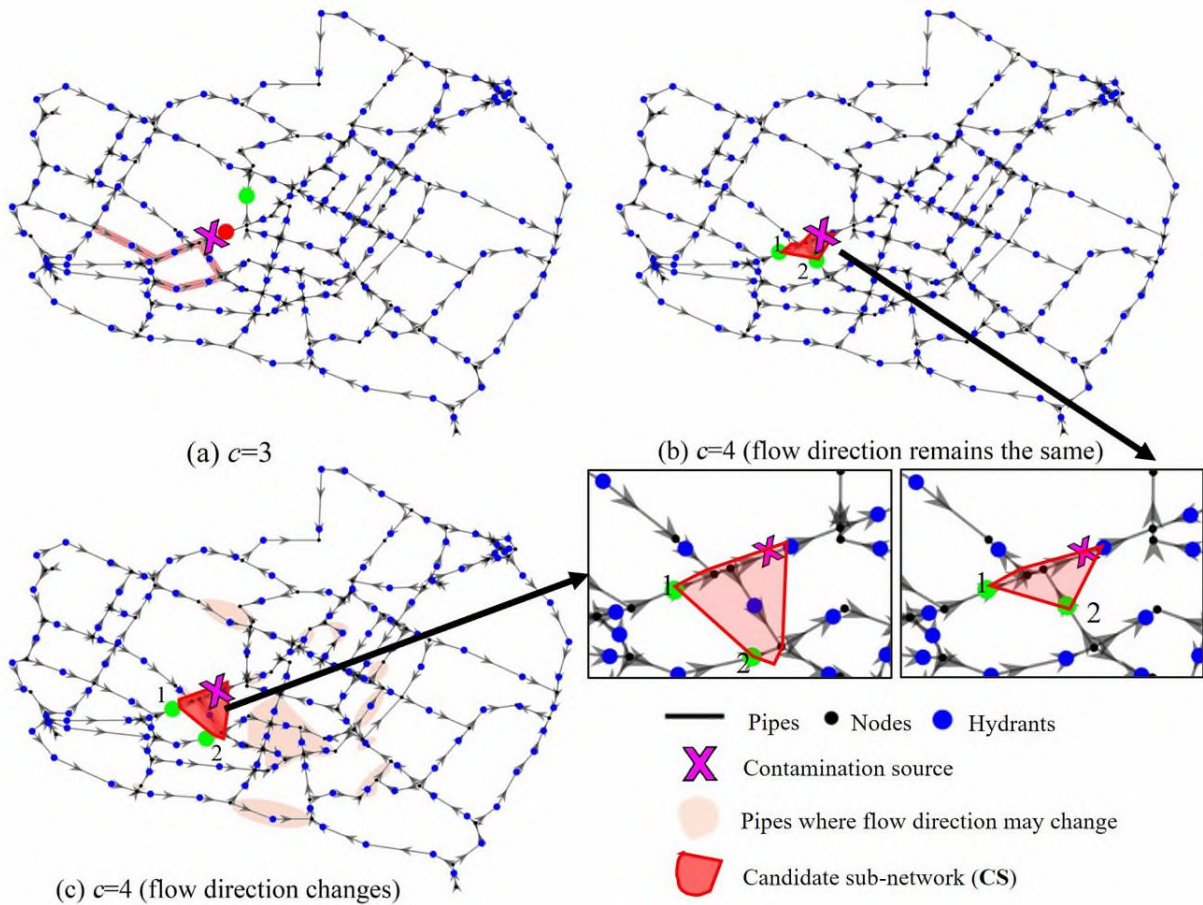


473

474

475

Figure 6: Source localization for the DMA case study with two contamination sources and two sampling locations at each cycle, where arrows indicate flow directions



476

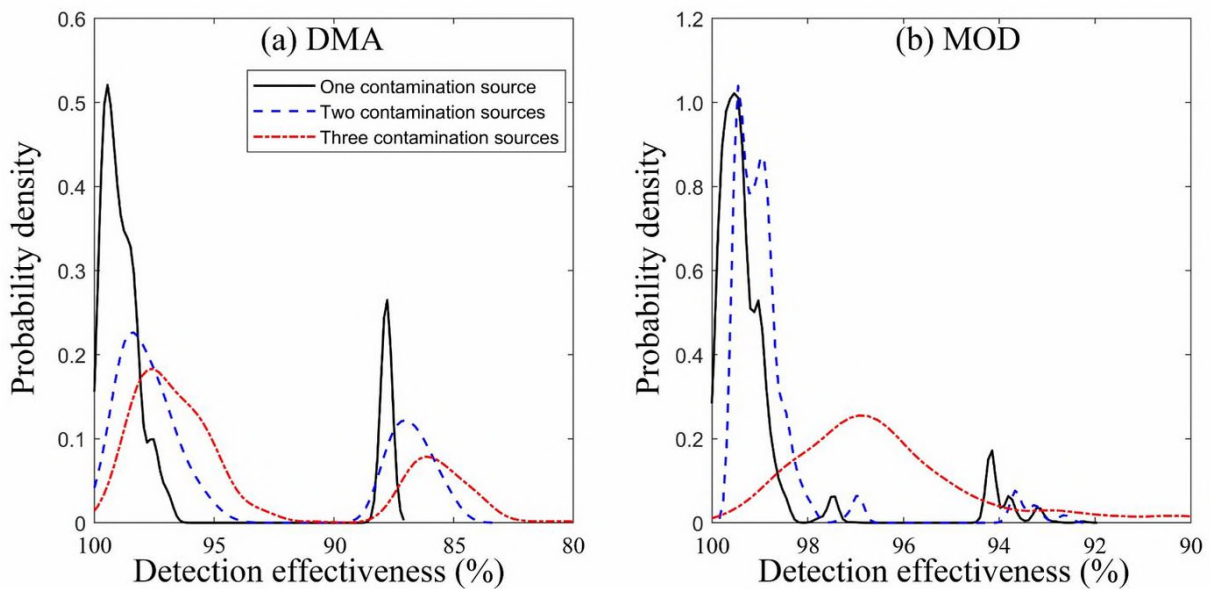
477 **Figure 7: Source localization for the MOD case study with one contamination source and two**
 478 **sampling locations at each cycle, where arrows indicate flow directions**

479 Figure 7 illustrates the proposed MGSM applied to the WDS with possible pipe flow changes. As
 480 shown in this figure, if the pipe flow directions do not change, the two sampling locations identified
 481 by the proposed MGSM are 1 and 2 (Figure 7b) based on the candidate sub-network (CS) determined
 482 at $c=3$ (Figure 7a). However, if the flow directions change after the sample tests at $c=3$, the CS for
 483 the next cycle needs to account for such variation. For the given example, one pipe is added to the
 484 CS due to its flow changing. This addition affects the optimal sampling locations selected by the
 485 MGSM (the location of 2 is changed as shown in Figure 7c). Based on this example, the flow
 486 direction changes can be easily handled by the proposed MGSM. For the MOD case study, we
 487 assume the change in the flow direction status occurs (Figure 7c) after $c=3$, followed by a change to
 488 the original direction of flow after another two cycles.

489 It is found that the proposed MGSM is able to identify the contamination sources for all scenarios
 490 considered in both case studies, implying its great effectiveness to localize contamination sources.
 491 In this study, we define a detection effectiveness (%) metric as follows,

$$\text{Detection effectiveness} = \left(1 - \frac{L_f}{L_{all}}\right) \times 100\% \quad (6)$$

492 Where L_f is the pipe length of the finally identified sub-network with contamination source(s) and
 493 L_{all} is the total pipe length of the entire WDS being considered. A high detection effectiveness
 494 represents that the proposed method can greatly reduce the efforts or budgets of the subsequent field
 495 investigations that are needed to micro-locate and eliminate contamination sources.



496
 497 **Figure 8: Detection effectiveness (%) of the proposed MGSM applied to the two case studies**

498 Figure 8 presents the probability density of the detection effectiveness (%) for all contamination
 499 scenarios considered, where the distribution of the ratio between the length of the finally identified
 500 pipes and the total pipe length of the WDS for all contamination events is presented. It is seen from
 501 this figure that the majority of the detection effectiveness (%) is higher than 95% and 98% for the
 502 DMA and MOD case study respectively. This indicates that the finally identified pipes with
 503 contamination source(s) represent a very small portion of the entire network, which can greatly
 504 improve the efficiency of the subsequent engineering effort to fix the contamination problem. The
 505 detection effectiveness (%) ranges between 80% and 90% for some contamination scenarios for the

506 DMA case study as shown in Figure 8(a). This is due to the sparse distribution of hydrants for these
507 events, and hence the length of the candidate sub-network identified by the proposed MGSM is
508 relatively large. The detection effectiveness (%) decreases when dealing with a larger number of
509 contamination sources that simultaneously exist in the WDS. It is noted that the detection
510 effectiveness (%) values are the same with those obtained using the average pipe length distance
511 between hydrants divided by the total pipe length of the network. This implies that the proposed
512 method is able to identify the pipe with contamination source between the two hydrants for each
513 scenario considered.

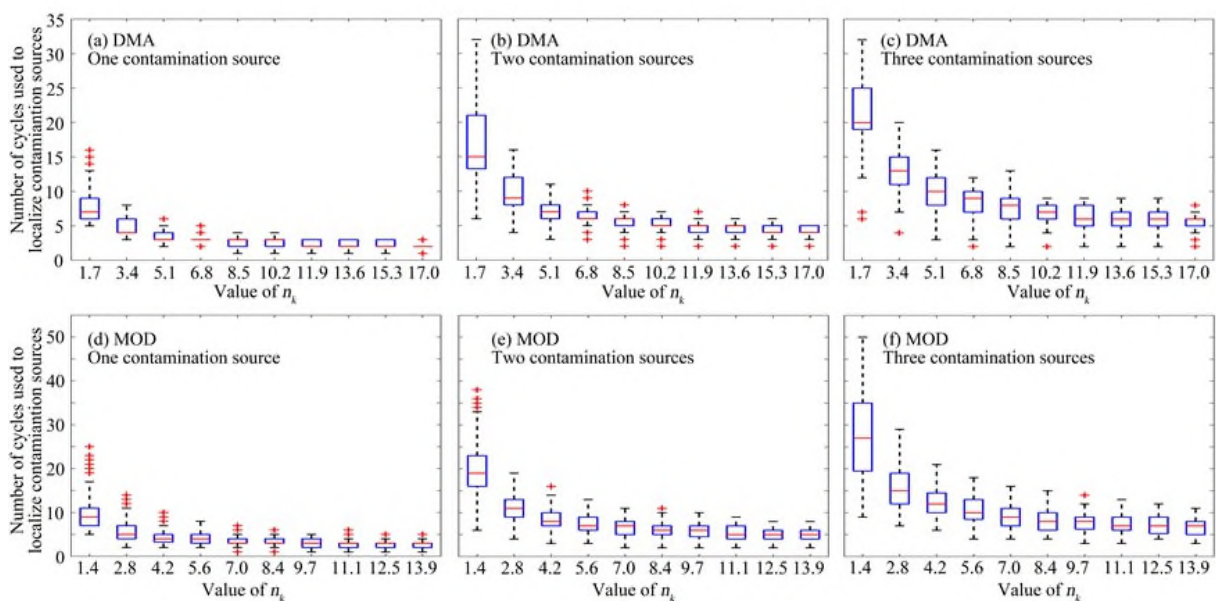
514 **4.2 Detection efficiency of the proposed MGSM**

515 The detection efficiency of the proposed MGSM can be evaluated using the number of total cycles
516 required for the entire procedure. The total time used in each cycle includes the time required to
517 collect and test samples, as well as the computation time needed to identify the sampling locations.
518 As previously stated, both the computation time and for sample collection are negligible compared
519 to the laboratory tests. Figure 9 shows the total number of cycles used to localize contamination
520 sources of the two case studies as a function of the varying number of samples per 100 km of pipe
521 length at each cycle (n_k), where $n_k = n/L_{tot} \times 100$. Such a normalization is used to enable the
522 generalization of the results to other WDSs.

523 As shown in Figure 9, an obvious trend that can be observed is that the detection efficiency is
524 improved when n increases for all different contamination scenarios (n_k ranges from about 1.5 to 5)
525 for both case studies. A significant increase in efficiency occurs for $n_k > 1.5$, with improvements
526 diminishing when $n_k > 6$. This is expected as a high n_k value indicates a larger number of available
527 teams for collecting samples and a significant laboratory capacity for simultaneously testing multiple
528 samples. The diminishing efficiency improvement for large n_k implies that an optimal sampling size
529 exists for the WDS when the efficiency is considered. For the DMA and MOD case studies, the
530 optimal n_k value can be between 7.0 and 8.5 as a further increase in n_k value does not significantly
531 improve the MGSM's detection efficiency, as shown in Figure 9. However, the optimal n_k value for
532 detection efficiency can be case study dependent as it can be related to the size of the WDS being

533 considered. In addition, a large n_k value corresponds to a significant financial commitment, and
 534 hence the decision process can be also affected by the budgets available.

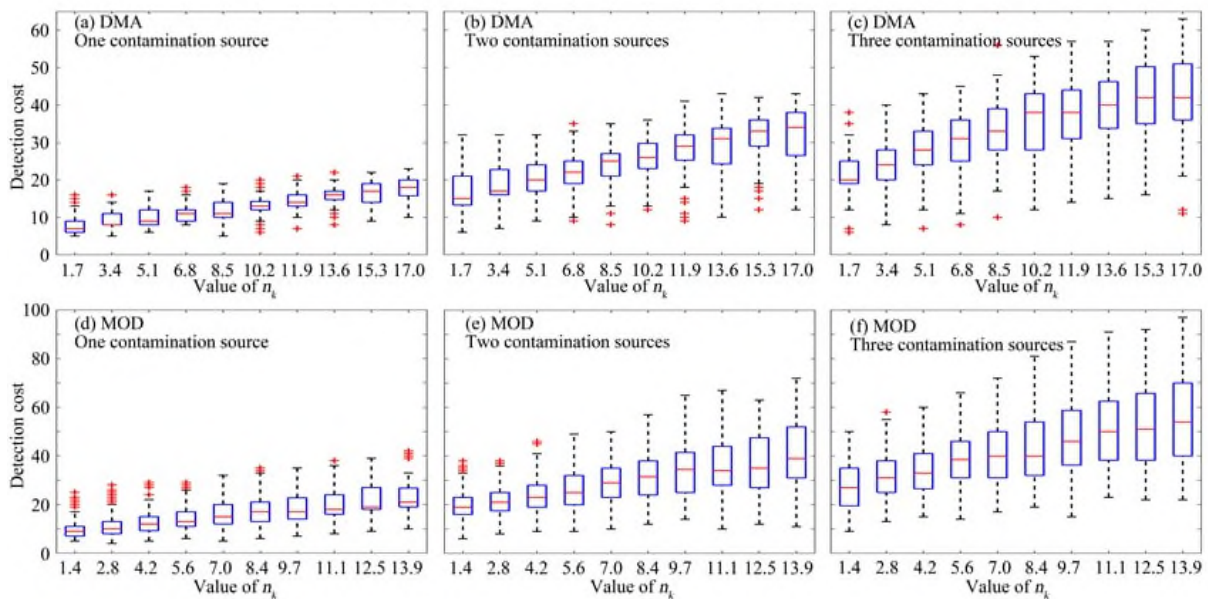
535 Interestingly, for the same number of sampling locations at each 100 km pipe length n_k , when n_k is
 536 relatively low, the total number of cycles can vary significantly. For example, for the DMA case
 537 study if $n_k=1.7$, the detection efficiency can vary from 5 to 15 cycles for the one contamination
 538 source, and range from 7 to 25 cycles when three contamination sources are simultaneously
 539 considered. Similar observations can be made for the MOD case study. This implies that the location
 540 of the contamination sources can appreciably affect the detection efficiency when there is a low
 541 number of sampling teams available and/or a limited laboratory capacity for testing multiple samples.
 542 When a sufficiently large n_k is considered, the detection efficiency variations become small, as
 543 observed in Figure 9. This implies that the choice of n_k will also affect the uncertainty associated
 544 with method efficiency, which should be also accounted for in engineering practice.



545
 546 **Figure 9: The number of cycles used to localize contamination sources versus the number of**
 547 **sampling points for every 100 km pipe length at each cycle (n_k) for the proposed MGSM**
 548 **applied to the two case studies**

549 **4.3 Detection cost of the proposed MGSM**

550 In this study, the detection cost of the proposed MGSM is measured by the total number of samples
 551 that have been tested to localize the contamination sources. Figure 10 shows the detection cost as a
 552 function of varying n_k for both case studies. Despite some variations, a large n_k value is generally
 553 associated with a greater detection cost for both case studies. In addition, the simultaneous presence
 554 of a larger number of contamination sources also causes an overall increase in detection costs. This
 555 information combined with the efficiency results in Figure 9 can be used as guidance for developing
 556 effective water quality sampling plans or budgets for a given WDS.



557
 558 **Figure 10: Detection cost (i.e., the number of total samples) versus the number of sampling**
 559 **points for every 100 km pipe length at each cycle (n_k) for the proposed MGSM applied to the**
 560 **two case studies**

561 5. Summary and Conclusions

562 Existing research on water quality management and contamination source localization in WDSs has
 563 focused mainly on developing methods that assume availability of accurate water quality models
 564 and multi-parameter online sensors. However, that is not true for many water utilities. A promising
 565 way to address such problems is through the iterative manual grab-sample strategies, thereby
 566 enabling effective contaminant localizing. To this end, this study proposes a new method for water

567 quality manual grab-sampling (termed as MGSM in this paper) to enable identification of
568 contamination sources in WDSs.

569 The proposed MGSM is suitable for situations where online multi-parameter water quality sensors
570 are sparsely available or completely missing, which is the case with many utilities. This is mainly
571 due to the high purchase and maintenance cost associated with these sensors, as well as their inability
572 (or inaccurate) to detect the complex water quality parameters (e.g., metals, microorganism and
573 personal care products, Jia et al. (2021b)). In addition, a grab-sampling method is tailored for the
574 cases when contamination is *continually* present in the WDS and with slow or low impacts to the
575 WDSs. That is the case with misconnections between water supply pipes and sewer (or grey) pipes
576 and contaminations caused by pipe leaks, corrosion or hydraulic turbulence. For events with serious
577 consequences, the candidate sub-networks (CSs) with contamination sources may need to be shut
578 down or sampled manually as much as possible.

579 Based on the results obtained for two real-world cases, the following findings and conclusions can
580 be drawn:

581 (1) The newly proposed MGSM can successfully detect and locate continuous contamination
582 source(s) for a wide range of scenarios, including multiple contamination source(s) in complex
583 WDSs with varying pipe flow directions. This is a significant advantage over the traditional
584 approach that works only with one contamination source and fixed flow directions, as described
585 in Wong et al. (2010).

586 (2) For the two case studies, the new MGSM identified contamination source(s) within 5% of
587 the total pipe length of the WDS. This indicates the high effectiveness of the proposed MGSM in
588 narrowing narrow down the spatial range of the sub-network with potential contamination sources.
589 From the practical point of view, it also improves the efficiency of maintenance efforts to eliminate
590 the sources of contamination.

591 (3) The detection efficiency (measured by the number of sampling and testing cycles) of the
592 MGSM can be significantly improved when the number of sampling points per 100 km pipe length
593 at each cycle (n_k) increases from about 1.5 to a moderate value (e.g. $n_k \approx 7$). The increase in
594 efficiency diminishes with further increases in n_k . This implies that there exists an optimal n_k value
595 for a given WDS, representing the balanced trade-off between detection efficiency and costs

596 associated with methodology. The detection cost grows with the increase in the number of sampling
597 points per 100 pipe length, n_k . All these findings are important for the implementation of the
598 method as they can guide the process of selecting the optimal number of sampling teams and
599 required laboratory capacity.

600 In view of the practical application, the proposed MGSM can be used to regularly check water
601 quality safety for WDSs with a low density of sensors as this is routine work in many water utilities.
602 For instance, in China, many water utilities need to take water samples from hydrants or end users
603 every month, with the number of samples depending on the scale of the WDS and importance level
604 of the city. These water samples are comprehensively measured in the laboratory following the
605 Water Quality Standard that has 106 parameters. Many water utilities collect grab samples from
606 large WDSs at fixed locations based on specialists' engineering expertise. For example, a
607 practitioner may collect grab samples from all established fixed locations (if say, 50 locations) and
608 test for a combination (or all) of the specified water quality parameters in the laboratory. Such a
609 strategy is time-consuming and expensive (labor and measurement costs). Therefore, the sampling
610 strategy can be improved with the aid of the proposed MGSM in order to save the cost. It can be
611 concluded that the MGSM is an alternative to the sensor-based detection methods.

612 The limitation of the method proposed here is the potentially high cost and time required to identify
613 the source(s) as all grab samples need to be collected manually (with technicians moving between
614 different locations during multiple cycles) and processed (in the lab). In addition, the pipes identified
615 as the potential contamination sources need to be inspected in the field to micro-locate the
616 contamination source(s) with the aid of manual checking or detection robots (Huang et al., 2020).
617 This too requires time and has a cost associated with it. This, however, applies to most of the existing
618 sensor-based methods as well. Another limitation is that the proposed MGSM can be only applicable
619 to contamination events with continuous injections to the WDS conditioned on known pipe flow
620 directions. Furthermore, when dealing with scenarios with pipe flow changes, there is likely that
621 such changes would affect the utility of the proposed MGSM, which needs attention within practical
622 implementation. While the practical application of the developed MGSM can be simple as it only
623 requires flow direction information (Zhang et al., 2021), it should be also acknowledged the flow
624 information can be challenging for some old pipes due to system uncertainties.

625 Future studies along this research line include (i) the application of the proposed method to further
626 large real WDSs; (ii) the extension of the graph partitioning strategy within the proposed MGSM to
627 account for both the pipe length and pipe velocity; (iii) the extension of the proposed MGSM to deal
628 with contamination events with intermittent injections to the WDS.

629 **Acknowledgements**

630 The corresponding author Professor Feifei Zheng was funded by the National Natural Science
631 Foundation of China (Grant No. 51922096), and Excellent Youth Natural Science Foundation of
632 Zhejiang Province, China (LR19E080003). Dr Weiwei Bi was funded by National Natural Science
633 Foundation of China (51808497). Dr. Huan-Feng Duan would like to appreciate the support from
634 the Hong Kong Research Grants Council (RGC) (project no. 15200719). Prof. Dragan Savic has
635 received funding from the European Research Council (ERC) under the European Union's Horizon
636 2020 research and innovation programme (Grant agreement No. 951424).

637 **References**

- 638 Asheri Arnon, T., Ezra, S. and Fishbain, B. (2019). Water characterization and early contamination
639 detection in highly varying stochastic background water, based on Machine Learning
640 methodology for processing real-time UV-Spectrophotometry. *Water Res.* 155, 333-342.
- 641 Bhatia, R. and Davis, C. (1995). A Cauchy-Schwarz inequality for operators with applications.
642 *Linear Algebra Appl.* 223-224, 119-129. Butera, I., Gómez-Hernández, J.J. and Nicotra, S.
643 2021. Contaminant-Source Detection in a Water Distribution System Using the Ensemble
644 Kalman Filter. *J. Water Resour. Plan. Manag.* 147(7), 04021029.
- 645 ChinaNews, (2020). <http://www.chinanews.com/sh/2020/07-30/9252169.shtml>.
- 646 Di Nardo, A., Giudicianni, C., Greco, R., Herrera, M., Santonastaso, G.F. and Scala, A. (2018).
647 Sensor placement in water distribution networks based on spectral algorithms. *13th*
648 *International Conference on Hydroinformatics (HIC2018)* 7.
- 649 Giudicianni, C., Herrera, M., Nardo, A.D., Greco, R., Creaco, E. and Scala, A. (2020). Topological
650 Placement of Quality Sensors in Water-Distribution Networks without the Recourse to
651 Hydraulic Modeling. *J. Water Resour. Plan. Manag.* 146(6), 04020030.
- 652 Grbčić, L., Lučin, I., Kranjčević, L. and Družeta, S. (2020). Water supply network pollution source
653 identification by random forest algorithm. *J. Hydroinformatics* 22(6), 1521-1535.

654 Hart, D., Rodriguez, J.S., Burkhardt, J., Borchers, B., Laird, C., Murray, R., Klise, K. and Haxton,
655 T. (2019). Quantifying Hydraulic and Water Quality Uncertainty to Inform Sampling of
656 Drinking Water Distribution Systems. *J. Water Resour. Plan. Manag.* 145(1), 04018084.

657 Hart, W.E. and Murray, R. (2010). Review of Sensor Placement Strategies for Contamination
658 Warning Systems in Drinking Water Distribution Systems. *J. Water Resour. Plan. Manag.*
659 136(6), 611-619.

660 He, G., Zhang, T., Zheng, F. and Zhang, Q. (2018). An efficient multi-objective optimization
661 method for water quality sensor placement within water distribution systems considering
662 contamination probability variations. *Water Res.* 143, 165-175.

663 He, G., Zhang, T., Zheng, F., Li, C., Zhang, Q., Dong, F. and Huang, Y. (2019) Reaction of
664 fleroxacin with chlorine and chlorine dioxide in drinking water distribution systems: Kinetics,
665 transformation mechanisms and toxicity evaluations. *Chem. Eng. J.* 374, 1191-1203.

666 Hu, C., Dai, L., Yan, X., Gong, W., Liu, X. and Wang, L. (2020). Modified NSGA-III for sensor
667 placement in water distribution system. *Inf. Sci.* 509, 488-500.

668 Hu, C., Ren, G., Liu, C., Li, M. and Jie, W. (2017). A Spark-based genetic algorithm for sensor
669 placement in large scale drinking water distribution systems. *Cluster Comput.* 20(2), 1089-
670 1099.

671 Hu, C., Zhao, J., Yan, X., Zeng, D. and Guo, S. (2015). A MapReduce based Parallel Niche Genetic
672 Algorithm for contaminant source identification in water distribution network. *Ad Hoc Netw.*
673 35, 116-126.

674 Huang, Y., Zheng, F., Kapelan, Z., Savic, D., Duan, H.-F. and Zhang, Q. (2020) Efficient Leak
675 Localization in Water Distribution Systems Using Multistage Optimal Valve Operations and
676 Smart Demand Metering. *Water Resour. Res.* 56(10), e2020WR028285.

677 Jerez, D.J., Jensen, H.A., Beer, M. and Broggi, M. (2021). Contaminant source identification in
678 water distribution networks: A Bayesian framework. *Mech. Syst. Signal Process* 159, 107834.

679 Jia, Y., Zheng, F., Zhang, Q., Duan, H.-F., Savic, D. and Kapelan, Z. (2021a). Foul sewer model
680 development using geotagged information and smart water meter data. *Water Res.* 204,
681 117594.

682 Jia, Y., Zheng, F., Maier, H.R., Ostfeld, A., Creaco, E., Savic, D., Langeveld, J. and Kapelan, Z.
683 (2021b) Water quality modelling in sewer networks: review and future research directions.
684 *Water Research*, 117419.

685 Khorshidi, M.S., Nikoo, M.R. and Sadegh, M. (2018). Optimal and objective placement of sensors
686 in water distribution systems using information theory. *Water Res.* 143, 218-228.

687 Li, C., Yang, R., Zhou, L., Zeng, S., Mavrovouniotis, M., Yang, M., Yang, S. and Wu, M. (2021).
688 Adaptive Multipopulation Evolutionary Algorithm for Contamination Source Identification
689 in Water Distribution Systems. *J. Water Resour. Plan. Manag.* 147(5), 04021014.

690 Maier, H.R., Kapelan, Z., Kasprzyk, J., Kollat, J., Matott, L.S., Cunha, M.C., Dandy, G.C., Gibbs,
691 M.S., Keedwell, E., Marchi, A., Ostfeld, A., Savic, D., Solomatine, D.P., Vrugt, J.A., Zecchin,
692 A.C., Minsker, B.S., Barbour, E.J., Kuczera, G., Pasha, F., Castelletti, A., Giuliani, M. and
693 Reed, P.M. (2014) Evolutionary algorithms and other metaheuristics in water resources:
694 Current status, research challenges and future directions. *Environ. Model Softw.* 62(0), 271-
695 299.

696 Mann, A.V., McKenna, S.A., Hart, W.E. and Laird, C.D. (2012). Real-time inversion in large-
697 scale water networks using discrete measurements. *Comput. Chem. Eng.* 37, 143-151.

698 Naserizade, S.S., Nikoo, M.R. and Montaseri, H. (2018). A risk-based multi-objective model for
699 optimal placement of sensors in water distribution system. *J. Hydrol.* 557, 147-159.

700 Ohar, Z., Lahav, O. and Ostfeld, A. (2015). Optimal sensor placement for detecting
701 organophosphate intrusions into water distribution systems. *Water Res.* 73, 193-203.

702 Oliker, N. and Ostfeld, A. (2014). A coupled classification – Evolutionary optimization model for
703 contamination event detection in water distribution systems. *Water Res.* 51, 234-245.

704 Ostfeld, A., Uber, J.G., Salomons, E., Berry, J.W., Hart, W.E., Phillips, C.A., Watson, J.-P., Dorini,
705 G., Jonkergouw, P., Kapelan, Z., Pierro, F.d., Khu, S.-T., Savic, D., Eliades, D., Polycarpou,
706 M., Ghimire, S.R., Barkdoll, B.D., Gueli, R., Huang, J.J., McBean, E.A., James, W., Krause,
707 A., Leskovec, J., Isovitsch, S., Xu, J., Guestrin, C., VanBriesen, J., Small, M., Fischbeck, P.,
708 Preis, A., Propato, M., Piller, O., Trachtman, G.B., Wu, Z.Y. and Walski, T. 2008. The Battle
709 of the Water Sensor Networks (BWSN): A Design Challenge for Engineers and Algorithms.
710 *J. Water Resour. Plan. Manag.* 134(6), 556-568.

711 Ostfeld, A., Oliker, N. and Salomons, E. (2014). Multiobjective Optimization for Least Cost
712 Design and Resiliency of Water Distribution Systems. *J. Water Resour. Plan. Manag.*
713 140(12), 04014037.

714 Preis, A. and Ostfeld, A. (2006). Contamination Source Identification in Water Systems: A Hybrid
715 Model Trees–Linear Programming Scheme. *J. Water Resour. Plan. Manag.* 132(4), 263-273.

716 Preis, A. and Ostfeld, A. (2007). A contamination source identification model for water
717 distribution system security. *Eng. Optim.* 39(8), 941-947.

718 Preis, A. and Ostfeld, A. (2008). Genetic algorithm for contaminant source characterization using
719 imperfect sensors. *Civ. Eng. Environ. Syst.* 25(1), 29-39.

720 Qi, Z., Zheng, F., Guo, D., Maier, H.R., Zhang, T., Yu, T. and Shao, Y. (2018). Better
721 Understanding of the Capacity of Pressure Sensor Systems to Detect Pipe Burst within Water
722 Distribution Networks. *J. Water Resour. Plan. Manag.* 144(7), 04018035.

723 Rathi, S. and Gupta, R. (2014). Sensor Placement Methods for Contamination Detection in Water
724 Distribution Networks: A Review. *Procedia Eng.* 89, 181-188.

725 Robertson, L., Gjerde, B., Hansen, E.F. and Stachurska-Hagen, T. (2008). A water contamination
726 incident in Oslo, Norway during October 2007; a basis for discussion of boil-water notices
727 and the potential for post-treatment contamination of drinking water supplies. *J. Water Health*
728 7(1), 55-66.

729 Rodriguez, J.S., Bynum, M., Laird, C., Hart, D.B., Klise, K.A., Burkhardt, J. and Haxton, T.,
730 (2021). Optimal Sampling Locations to Reduce Uncertainty in Contamination Extent in
731 Water Distribution Systems. *J. Infrastruct. Syst.* 27(3), p.04021026.

732 Sankary, N. and Ostfeld, A. (2018). Multiobjective Optimization of Inline Mobile and Fixed
733 Wireless Sensor Networks under Conditions of Demand Uncertainty. *J. Water Resour. Plan.*
734 *Manag.* 144(8), 04018043.

735 Sankary, N. and Ostfeld, A. (2019). Bayesian Localization of Water Distribution System
736 Contamination Intrusion Events Using Inline Mobile Sensor Data. *J. Water Resour. Plan.*
737 *Manag.* 145(8), 04019029.

738 Sun, L., Yan, H., Xin, K. and Tao, T. (2019). Contamination source identification in water
739 distribution networks using convolutional neural network. *Environ. Sci. Pollut. Res.* 26(36),
740 36786-36797.

741 Tinelli, S., Creaco, E. and Ciaponi, C. (2017). Sampling Significant Contamination Events for
742 Optimal Sensor Placement in Water Distribution Systems. *J. Water Resour. Plan. Manag.*
743 143(9), 04017058.

744 Ung, H., Piller, O., Gilbert, D. and Mortazavi, I. (2017). Accurate and Optimal Sensor Placement
745 for Source Identification of Water Distribution Networks. *J. Water Resour. Plan. Manag.*
746 143(8), 04017032.

- 747 Vrachimis, S.G., Lifshitz, R., Eliades, D.G., Polycarpou, M.M. and Ostfeld, A. (2020). Active
748 Contamination Detection in Water-Distribution Systems. *J. Water Resour. Plan. Manag.*
749 146(4), 04020014.
- 750 Weickgenannt, M., Kapelan, Z., Blokker, M. and Savic, D.A. (2010). Risk-Based Sensor
751 Placement for Contaminant Detection in Water Distribution Systems. *J. Water Resour. Plan.*
752 *Manag.* 136(6), 629-636.
- 753 Winter, C.d., Palleti, V.R., Worm, D. and Kooij, R. (2019). Optimal placement of imperfect water
754 quality sensors in water distribution networks. *Comput. Chem. Eng.* 121, 200-211.
- 755 Wong, A., Young, J. and Laird, C.D. (2010). Optimal determination of grab sample location and
756 source inversion in large-scale water distribution systems. *Water Distribution Systems*
757 *Analysis 2010*.
- 758 Yang, X. and Boccelli, D.L. (2014). Bayesian Approach for Real-Time Probabilistic
759 Contamination Source Identification. *J. Water Resour. Plan. Manag.* 140(8), 04014019.
- 760 Yang, X. and Boccelli, D.L. (2016). Model-Based Event Detection for Contaminant Warning
761 Systems. *J. Water Resour. Plan. Manag.* 142(11), 04016048.
- 762 Zhang, Q., Zheng, F., Jia, Y., Savic, D. and Kapelan, Z. (2021) Real-time foul sewer hydraulic
763 modelling driven by water consumption data from water distribution systems. *Water Res.* 188,
764 116544.
- 765 Zhang, Q., Zheng, F., Kapelan, Z., Savic, D., He, G. and Ma, Y. (2020) Assessing the global
766 resilience of water quality sensor placement strategies within water distribution systems.
767 *Water Res.* 172, 115527.
- 768 Zheng, F., Du, J., Diao, K., Zhang, T., Yu, T. and Shao, Y. (2018). Investigating Effectiveness of
769 Sensor Placement Strategies in Contamination Detection within Water Distribution Systems.
770 *J. Water Resour. Plan. Manag.* 144(4), 06018003.